MEMRI Monitoring of Manganese Release and Transport in the Rat Brain Following Convection-Enhanced Delivery (CED) of Manganese (III)-Transferrin

C. H. Sotak[1,2], and A. P. Koretsky[3]
[1]Biomedical Engineering, Worcester Polytechnic Institute, Worcester, MA, United States, [2]Radiology, University of Massachusetts Medical School, Worcester, MA, United States, [3]NINDS/LFMI, National Institutes of Health, Bethesda, MD, United States

Introduction: Manganese (Mn^{2+}) has been widely used as a T_1-weighted MR contrast agent for functional imaging (1), neuronal tract tracing (2), and as an anatomical contrast agent (3). Manganese-enhanced MRI (MEMRI) methods generally detect Mn^{2+} in its role as a Ca^{2+} analogue; however, Mn^{2+} delivery into cells can also be achieved when manganese mimics other biometals such as iron (4). In this case, transferrins (Tf) – a major class of plasma iron-binding proteins – can form a metal-Tf complex with manganese, which is then transported across the cell membrane via transferrin-receptor-1 (TfR1) – mediated endocytosis. Subsequent acidification within the endosome releases manganese from the metalloprotein. The free Mn^{3+} is rapidly reduced to its more stable divalent form and then transported across the endosomal membrane into the cytosol. The metal-free apo-Tf/TfR1 complex remaining within the endosome is recycled back to the cell surface and dissociates for reuse in another cycle of cellular metal-ion uptake. The cyclical nature of this process can potentially label cells with relatively high concentrations of Mn^{2+} and the *in vitro* feasibility of this approach has been demonstrated by labeling murine hepatocytes with Mn^{2+} via incubation in Mn(III)-Tf (5). In this study, MEMRI was used to monitor the *in vivo* release and transport of manganese in the rat brain following convection-enhanced delivery (CED) (6) of Mn(III)-Tf. The spatio-temporal evolution of MEMRI signal enhancement and T_1 relaxation times were evaluated for a range of Mn(III)-Tf doses and infusion periods. The same experimental protocol was repeated using CED of Mn^{2+} to establish the similarities and differences between the enhancement and transport properties of the two contrast agents.

Methods: *Synthesis*: Mn(III)-Tf was prepared by a modified procedure of Aisen *et al.* (7). *CED of Mn(III)-Tf* (6): Infusion volumes (5-20 µL) of either Mn(III)-Tf or Mn^{2+}, with varying concentrations (0.66-4.0 mM), were delivered into the rat striatum over a range of time periods (25-200 min) via intracerebral cannula. *MRI*: MRI was performed at 7.0T using a Bruker Biospec with a Pharmascan magnet. Multi-slice, T_1-weighted (T_1-WT) MR images (TR/TE = 500/15.9 ms) were acquired over a range of time periods (0.5 – 73 h) following the CED period**.** Other imaging parameters were: FOV = 25.6 mm X 25.6 mm; data acquisition matrix = 256 X 128 (zero-filled to 256 X 256); NEX = 8; and 1-mm-thick slices. Data for calculating T_1 maps were acquired with the same FOV, data acquisition matrix, and slice thickness at interleaved time points between the T_1-WT scans. The temporal evolution of the T_1 relaxation times was evaluated in the contrast-enhanced region (and the homologous contralateral ROI) for the injection slice in each animal. The T_1 relaxation data for all of the animals in each group were then pooled to generate separate T_1 time-series plots for the respective Mn(III)-Tf- and Mn^{2+}-treated groups.

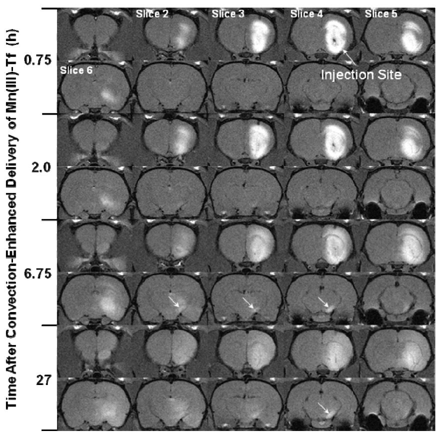

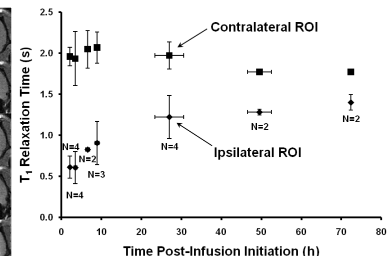

Fig. 1. Left – Ten-slice, T_1-WT data sets as a function of time after 100-min CED of 20 µL of 655 mM Mn(III)-Tf. **Above** – Plot of *in vivo* T_1 relaxation times within the ipsilateral contrast-enhanced ROI – and the homologous contralateral ROI – of the injection slice versus time following CED of Mn(III)-Tf. N is the number of animals evaluated at each time point.

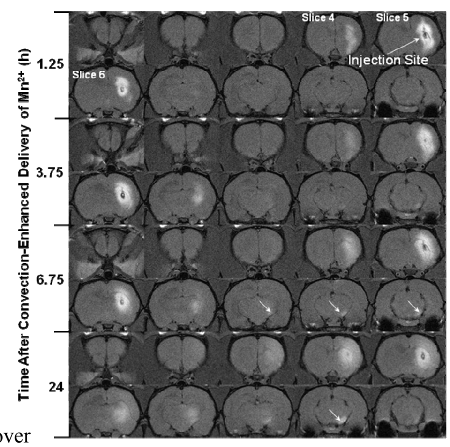

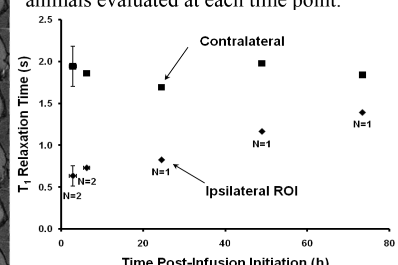

Fig. 2. Left – Ten-slice, T_1-WT data sets as a function of time after 25-min CED of 5 µL of 4.0 mM Mn^{2+}. **Above** – Plot of *in vivo* T_1 relaxation times within the ipsilateral contrast-enhanced ROI – and the homologous contralateral ROI – of the injection slice versus time following CED of Mn^{2+}. N is the number of animals evaluated at each time point.

Results and Discussion: Fig. 1 (Left) shows a series of T_1-WT data sets as a function of time after 100-min CED of 20 µL of 655 mM Mn(III)-Tf. At 0.75 h following the CED period, T_1-WT image enhancement was apparent in Slices 2-6. Over time, the region of T_1-WT image enhancement expanded both within and between slices. By 6.75 h, T_1-WT hyperintensity had migrated at least 5 mm from the injection site; tracing the striatonigral neuronal tract indicted by the arrows in the 6.75-h image set. By 27 h, the T_1-WT hyperintensity was dispersed over 9/10 of the slices shown and remained conspicuous in the substantia nigra (SN) (arrow in 27-h image set). Fig. 1 (Above) shows the temporal evolution of the T_1 relaxation times within the ipsilateral contrast-enhanced ROI – and the homologous contralateral ROI – for the injection slice for the Mn(III)-Tf-infusion group. At the earliest time point, the mean ipsilateral T_1 values declined by 69% relative to the homologous contralateral ROI ($P < 0.001$; Student's paired t-test) and then returned to near baseline over the next 72 h. Fig. 2 shows a series of T_1-WT MEMRI data sets as a function of time after 25-min CED of 5 µL of 4 mM Mn^{2+}. At 1.25 h following the CED period, T_1-WT image enhancement was apparent in only three slices (4-6) because of the smaller injection volume relative to that used for the Mn(III)-Tf-treated animal. Nevertheless, by 6.75 h, the T_1-WT hyperintensity had still migrated at least 5 mm from the injection site; tracing the striatonigral neuronal tract indicted by the arrows in the 6.75-h image set. This observation was analogous to that observed for Mn(III)-Tf in the 6.75-h image set. By 24 h, the T_1-WT hyperintensity was dispersed over 8/10 of the slices shown and remained conspicuous in the SN (arrow in 24-h image set). Fig. 2 (Above) shows the temporal evolution of the T_1 relaxation times within the ipsilateral contrast-enhanced ROI – and the homologous contralateral ROI – for the injection slice for the Mn^{2+}-infusion group. At the earliest time point, the mean ipsilateral T_1 values declined by 67% relative to the homologous contralateral ROI ($P < 0.05$) and then returned to near baseline over the next 73 h.

Conclusions: CED of Mn(III)-Tf into the rat brain enabled the subsequent investigation of its properties as an *in vivo* MRI contrast agent. The spatio-temporal evolution of MEMRI signal enhancement and T_1 relaxation times following Mn(III)-Tf infusion was comparable to that observed following CED of Mn^{2+} alone as well as results from $^{54}Mn^{2+}$ radioisotope studies for *in vivo* rat brain (8). Furthermore, Mn^{2+} released following intrastriatal Mn(III)-Tf infusion was transported along the striatonigral pathway and the temporal dynamics are in excellent agreement with the neuronal tract tracing studies that employ Mn^{2+} alone and literature results based on radiotracer studies. The results of this study are consistent with the release and subsequent transport of Mn^{2+} following receptor-mediated endocytosis of Mn(III)-Tf.

References: 1. Lin Y, Koretsky AP. Magn Reson Med 1997;38:378. 2. Pautler RG, Silva AC, Koretsky AP. Magn. Reson. Med 1998;40:740. 3. Pautler RG. Methods Mol Med 2006;124:365. 4. Malecki EA, et al. J Neurosci Res 1999;56:113. 5. Sotak CH, Sharer K, Koretsky AP. Contrast Media Mol Imaging 2008;3:95. 6. Chen YM, et al. J Neurosurg 1999;90:315. 7. Aisen P, et al. J Biol Chem 1969;244:4628. 8. Sloot WN, Gramsbergen J-BP. Brain Res 1994;657:124. This research was supported by the Intramural Research Program of the National Institutes of Health (NIH) and the National Institute of Neurological Disorders and Stroke (NINDS).